Electrostatic thermal noise in a weakly ionized collisional plasma

M. Martinović, A. Zaslavsky, M. Maksimović, S. Šegan

Electrostatic thermal noise in a weakly ionized collisional plasma

M. M. Martinović[1,2,3], A. Zaslavsky[1], M. Maksimović[1] ID, and S. Šegan[2]

[1]LESIA, Observatoire de Paris, UPMC, Université Paris Diderot, CNRS, Meudon, France, [2]Department of Astronomy, Faculty of Mathematics, ,Belgrade, Serbia, [3]IHIS Techno-experts d.o.o. – Research and Development Center, Belgrade, Serbia

Abstract Quasi-thermal noise (QTN) spectroscopy is a plasma diagnostic technique which enables precise measurements of local electron velocity distribution function moments. This technique is based on measurements and analysis of voltage fluctuations at the antenna terminals, induced by thermal motion of charged particles. In this work, we accommodate, for the first time, this technique to weakly ionized collisional plasmas. It turns out that the QTN spectrum is modified both at low frequencies, increasing the level of power spectrum, and around the plasma frequency, where collisions damp the plasma oscillations and therefore broaden and reduce the amplitude of so called "plasma peak," while the spectrum at high frequencies is nearly unmodified compared to the collisionless case. Based on these results, we show that QTN spectroscopy enables independent measurements of the collision frequency, electron density, and temperature, provided the ratio of collision frequency to plasma frequency is $\nu/\omega_p \sim 0.1$. The method presented here can be used for precise estimation of plasma parameters in laboratory devices and unmagnetized ionospheres, while application in the ionosphere of Earth is possible but limited to small, low-frequency range due to magnetic field influence.

1. Introduction

A passive electric antenna immersed in a stable plasma and connected to a sensitive wave receiver is able to detect thermal fluctuations of the electric field due to the motion of plasma electrons and ions. The power spectra measured this way at the antenna terminals can be analyzed using quasi-thermal noise (QTN) spectroscopy [*Meyer-Vernet*, 1979] to accurately determine plasma density and temperature. This technique has been widely used for in situ space plasma diagnostics in both solar wind and planetary magnetospheres [see, e.g., *Moncuquet et al.*, 2005; *Le Chat et al.*, 2011], that is, in nearly perfectly collisionless plasma.

On the other hand, laboratory and ionospheric plasmas (especially at lower ionospheric layers) dominantly consist of neutral atoms and molecules, which frequently collide with electron population. The antenna impedance in a collisional plasma has been theoretically treated in the hydrodynamic approximation (which is reliable above the plasma frequency) by *Balmain* [1964] and measured in various rocket [see, e.g., *Hoang*, 1972; *Spencer and Patra*, 2015] and laboratory experiments [see, e.g., *Hall and Landauer*, 1971; *Blackwell et al.*, 2007a, 2007b]. This paper uses kinetic approach to examine the influence of collisions. Therefore, it proposes a treatment valid below the plasma frequency, which was not the case for the hydrodynamic models. As we shall see, collisions induce measurable effects on the QTN spectrum.

In section 2 we calculate QTN generic spectrum for collisional plasma and explore some of its features for wire dipole antennas. Another antenna geometry widely used is the one with double-sphere antennas which is not investigated in detail in this paper for two reasons. First, these two commonly used geometries show very similar behavior of the QTN spectra for $\omega \lesssim \omega_p$, with only some quantitative differences [*Meyer-Vernet and Perche*, 1989], and it is also the case for corrections due to collisions. Second, it is well known that shot noise [*Meyer-Vernet*, 1983] overwhelms the signal on sphere antennas at low frequencies. This problem is present whenever the antenna potential is not both negative and large compared to the electron thermal energy [*Martinović*, 2016], while the low potential value, as will be shown below, increases the accuracy of our technique. This is why spherical dipoles are usually avoided in the QTN measurements.

In section 3 we investigate the applicability of our theory to ionospheric and laboratory plasmas. Magnetic field in the ionosphere of Earth causes fundamental modifications to the entire spectrum. Because of this, usage of the QTN kinetic collisional theory for unmagnetized plasma is still possible, but is strictly limited
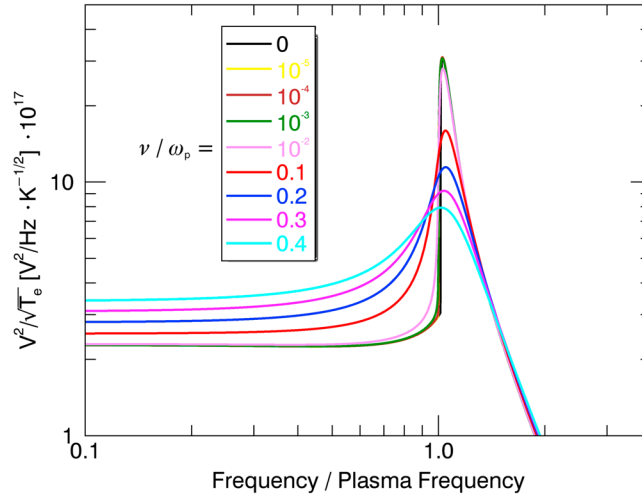
Figure 1. QTN power spectra observed by a long wire dipole antenna ($L_{ant}/L_D = 16$) for different values of the collision frequency. Result for $\nu = 0$ is identical as the one from *Meyer-Vernet and Perche* [1989].

to very low frequencies. We further deal with problems in real laboratory plasmas, defining the conditions for which the theory is valid and usable in experiments. It is concluded that absolute value of the antenna potential should be as low as possible in order to avoid unwanted effects of the plasma sheath, while usage of tiny dipoles is obligatory in order to preserve the simple form of the antenna current distribution.

2. Quasi-Thermal Noise in Collisional Plasmas

For plasmas in thermal equilibrium the thermal noise power spectrum is described by Nyquist's formula [*Nyquist*, 1928]:

$$V^2(\omega) = 4k_b T_e Re[Z(\omega)] \tag{1}$$

where k_b and T_e are the Boltzmann constant and electron kinetic temperature. $Z(\omega)$ is the antenna impedance, given by

$$Z(\omega) = \frac{4i}{\pi^2 \epsilon_0 \omega} \int_0^\infty \frac{F\left(kL_{ant}\right)}{\epsilon(k,\omega)} dk \tag{2}$$

Here k is wave number and $F(kL_{ant})$ is the antenna response function, determined by the current distribution and geometry of the antenna. For a tiny dipole with infinitesimal gap between its arms and triangular current distribution, it is given as [*Kuehl*, 1966]

$$F(x) = (x)^{-1} \left[Si(x) - \frac{1}{2}Si(2x) - \frac{2}{x} \sin^4 \frac{x}{2} \right] J_0^2 \left(x \frac{a_{ant}}{L_{ant}} \right) \tag{3}$$

with L_{ant} and a_{ant} being antenna length and radius.

Plasma dielectric function $\epsilon(\omega, \vec{k})$ can be obtained for collisional, weakly ionized plasma using Vlasov equation and collision term given by *Bhatnagar et al.* [1954]. Assuming that equilibrium velocity distribution function (VDF) is Maxwellian, we obtain [*Alexandrov et al.*, 1984]

$$\epsilon(k,\omega) = 1 + \frac{1}{k^2 L_D^2} \frac{1 + (z + i\nu')Z_0(\zeta)}{1 + i\nu' Z_0(\zeta)} \tag{4}$$

Here we use substitutions $\zeta = z + i\nu'$, $z = \omega/kv_{the}$, $\nu' = \nu/kv_{the}$, where $Z_0(\zeta)$ is the plasma dispersion function [*Fried and Conte*, 1961], $v_{the} = \sqrt{2k_b T_e/m_e}$ is the electron thermal velocity, and $L_D = 2^{-1/2}v_{the}/\omega_p$ is the Debye length. The angular plasma frequency is given as $\omega_p = \sqrt{n_e e^2/\epsilon_0 m_e}$ (with n_e, e, and m_e being electron density, charge, and mass, respectively, and ϵ_0 is dielectric permittivity of vacuum).

Using equation (1) the thermal noise can be calculated numerically and is shown on Figure 1. It is noticeable that the plasma peak is damped and that its location in the spectrum is slightly varying. Both features are important when $\nu/\omega_p > 10^{-2}$ and can be directly used for measurement of electron density, temperature, and collision frequency if the spectral resolution is satisfactory. The low-frequency part of the spectrum is evidently increased for $\nu/\omega_p > 0.1$, and this effect is important to take into account in order to avoid overestimation of the electron temperature when it is examined by using the "thermal plateau" [*Meyer-Vernet and Perche*, 1989] below ω_p. On the other hand, the high-frequency part is almost completely unmodified by collisions. It is important to note that the trend shown on Figure 1 is commonly present for long dipoles and change in the L_{ant}/L_D parameter only changes the peak to plateau signal ratio (see section 2.3 for details). We give the closer insight below for each of these spectral domains.
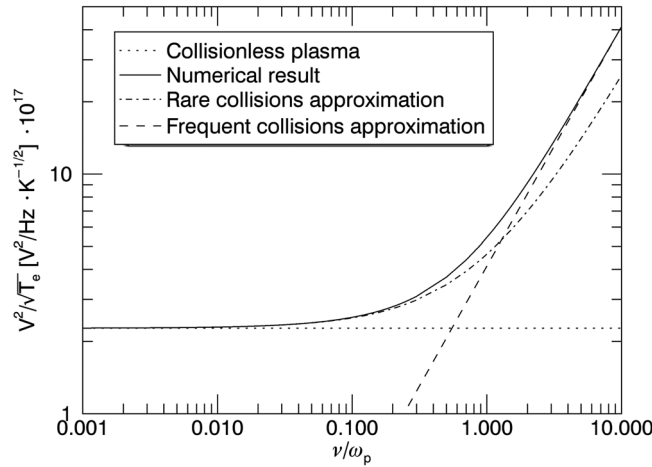
Figure 2. Level of the QTN on a wire dipole antenna ($L_{ant}/L_D = 16$) at $\omega = 0.01\omega_p$ computed numerically using equation (7) and first-order approximations given by equations (9) and (10).

2.1. Low-Frequency Limit

If we write the plasma dispersion function in the form of the imaginary error function as

$$Z_0(\zeta) = \pi^{1/2}e^{-\zeta^2}[-erfi(\zeta) + i] \quad (5)$$

it can be approximated by series for small values of z as

$$Z_0(\zeta) \approx i\pi^{-1/2}e^{\nu'^2}erfc(\nu') - 2z - 2i\nu'z^2 + ... \quad (6)$$

where $erfc(x)$ stands for the complementary error function. Putting equation (6) into (4) and then into equation (2), after some tedious calculations, we have

$$Re[Z(\omega)]_{\nu\to 0} = \sqrt{\frac{8}{\pi^3}} \frac{L_D}{\epsilon_0\omega_p} \int_0^\infty \frac{kF\left(kL_{ant}\right)}{\left[1 + k^2L_D^2\right]^2} M\left(\nu'\right) dk \quad (7)$$

The result obtained is the same as for the case of collisionless plasma up to a factor

$$M\left(\nu'\right) = \frac{e^{\nu'^2}erfc\left(\nu'\right)}{\left[1 - \nu'\pi^{1/2}e^{\nu'^2}erfc\left(\nu'\right)\right]} \quad (8)$$

in the integrand. This term represents the affection of collisions and can be simplified for small values of ν' as

$$M(\nu')_{\nu'\to 0} \approx 1 + \pi^{-1/2}(\pi - 2)\nu' + (\pi - 3)\nu'^2 + ... \quad (9)$$

Comparison with numerical results is shown on Figure 2. It is worth noting that using only the first term from equation (9) gives error less than 0.15% for $\nu/\omega_p < 10^{-2}$ and less than 2% for $\nu/\omega_p \sim 0.3$ compared with the precise value of the QTN calculated using equation (4), while the computation time differs for a factor of ~ 20. The approximate expression is valid for the entire frequency range below ω_p.

In the collisionless limit, $\nu = 0$ implies $M = 1$, and we turn back to the well-known expression that can be derived using the usual Debye screening dielectric function $\epsilon\left(\omega, \vec{k}\right) = 1 + \left(kL_D\right)^{-2}$.

The factor M can also be approximated for large values of ν' to be

$$M\left(\nu'\right)_{\nu\to\infty} \approx 2\pi^{-1/2}\left(\nu' + \nu'^{-1}\right) + ... \quad (10)$$

and for frequent collisions, we have

$$Re[Z(\omega, \nu)]_{\nu\to\infty} = \frac{4}{\pi^2\epsilon_0} \frac{\nu}{\omega_p^2} \int_0^\infty \frac{F\left(kL_{ant}\right)}{\left[1 + k^2L_D^2\right]^2} dk \quad (11)$$

yielding clear linear increase of the power spectrum level with ν, while the integrand is not depending on the collision frequency. Using equation (11) gives uncertainty less than 5% for $\nu/\omega_p > 4$ and less than 1% for $\nu/\omega_p > 8.5$. These estimates are correct for $\omega/\omega_p < 0.1$. Above these frequencies, the approximation causes errors above 20% and is not useful for quick estimation of temperature or collision frequency.

2.2. High Frequencies $\omega > \omega_p$

High-frequency part of the QTN spectrum is directly proportional to the plasma pressure and can be used to determine the plasma temperature [see, e.g., *Issautier et al.*, 1999; *Le Chat et al.*, 2011]. How is this modified by the collisions?

In the high-frequency (hydrodynamic) limit, we can develop the expression for dielectric permittivity by developing equation (4) in series for $z \to \infty$ [*Fried and Conte*, 1961] and keeping only terms of the zeroth and first order in ν/ω to obtain the result

$$\epsilon(\omega, k) = 1 - \frac{\omega_p^2}{\omega^2 - i\omega\nu - (3/2)k^2 v_{\text{the}}^2} \tag{12}$$

This expression is equivalent to the one obtained by using the linearized hydrodynamic equations with a pressure term $p_e = 3n_e k_b T_e$. Also, by omitting the last term in the denominator we converge to the well-known result for a cold plasma [*Balmain*, 1964]. Using equation (12), the integral in equation (2) can be calculated analytically, giving

$$Z(\omega) = \frac{2F\left(k_* L_{\text{ant}}\right)}{3\pi\epsilon_0 \omega L_D^2 k_*} \tag{13}$$

with complex pole

$$k_* = \frac{1}{L_D}\sqrt{\frac{1}{3}\left(\frac{\omega^2}{\omega_p^2} - 1 - i\frac{\omega\nu}{\omega_p^2}\right)} \tag{14}$$

From equation (14) it is notable that if $\omega - \omega_p \gg \nu$, then $k_* \approx \left(\sqrt{3}L_D\right)^{-1}\left(\omega^2/\omega_p^2 - 1\right)^{1/2}$ and the level of high-frequency part of the spectrum is independent of ν. This means that the expressions given at *Meyer-Vernet and Perche* [1989] stay valid for high frequencies. This also implies that expressions given by *Chateau and Meyer-Vernet* [1991] for long antennas can be used to quickly estimate T_e from the level of high-frequency part of the spectrum.

2.3. Resonance Region $\omega \sim \omega_p$

Around the plasma frequency the hydrodynamic approach described by equation (13) gives only approximate results, and full QTN expression that includes equation (4) needs to be used.

Since the location of the plasma peak (depending mostly of n_e and very slightly of T_e) is shifted due to collisions, this effect needs to be taken into account for an accurate estimation of the electron density. On the other hand, damping of the plasma oscillations near the plasma frequency will result in sharp decrease of the signal at the peak if $\nu/\omega_p > 10^{-2}$. The comparison of the peak and the low-frequency thermal plateau intensities is illustrating this effect. Both of these parameters are numerically calculated for multiple values of ν/ω_p in the L_{ant}/L_D range of interest and given on Figure 3. For $\nu/\omega_p > 0.5$, the plasma peak completely disappears from the spectrum and is not practically useful for estimation of n_e.

2.4. Antenna Capacitance

We define the antenna capacitance as $C_{\text{ant}} = 1/\omega Im[Z(\omega)]$. In order to examine the imaginary part of the antenna impedance at low frequencies, we perform a similar calculation as in section 2.1 to obtain a simple expression $Re\left[(\epsilon(\omega, k))^{-1}\right]_{\omega\to 0} = \left(1 + (kL_D)^{-2}\right)^{-1}$, identical to the collisionless case. Similarly, for the high-frequency part of the spectrum the hydrodynamic treatment described in section 2.2 can be used, again concluding that collisions do not affect high-frequency spectrum. This implies that well-known analytical expressions for both dipole and spherical antennas [see e.g. *Schelkunoff and Friis*, 1952; *Balanis*, 1997] are still valid in both low- and high-frequency limit.

On the other hand, for $\omega \sim \omega_p$ the antenna capacitance increases and is strongly peaked at the plasma frequency for $L_{\text{ant}}/L_D > 5$ [*Schiff*, 1970; *Nakatani and Kuehl*, 1976]. The effect of collisions is visible through "damping" of the plasma oscillations in similar way as for the QTN spectra, with the peak disappearing for $\nu/\omega_p > 0.1$. Example of the dipole antenna capacitance in a collisional plasma is given at Figure 4 showing that the collisional effects become important for $\nu/\omega_p \geq 10^{-2}$.

3. Practical Consequences

The QTN spectroscopy is routinely used in the solar wind and planetary magnetospheres, providing independent measurements of the electron density and temperature. These plasmas are practically collisionless, while ionospheric and laboratory plasmas have considerable amount of neutral atoms and molecules that collide with electrons and can affect the power spectra of the QTN in the way described in section 2. In order
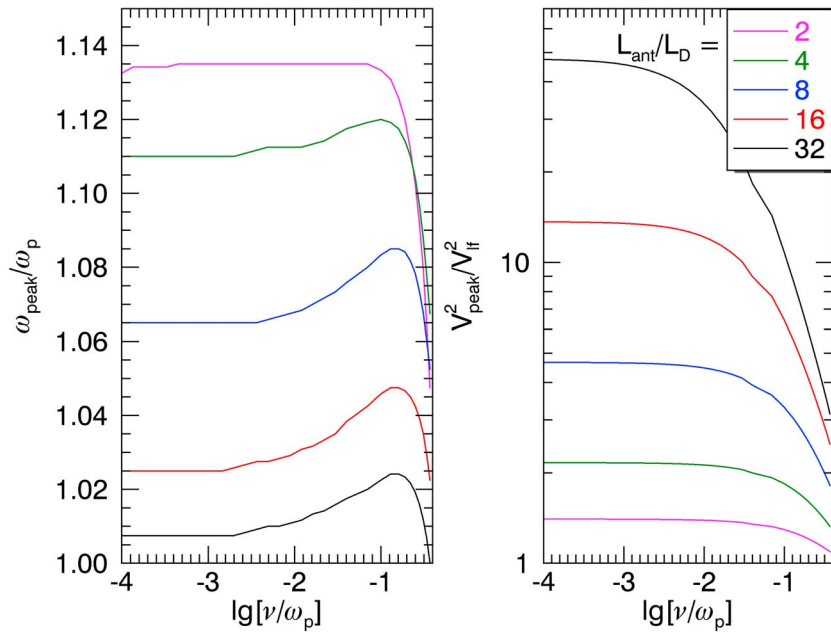
Figure 3. (left) Location and (right) intensity of the plasma peak observed by a wire dipole antenna in collisional plasma for some of L_{ant}/L_D ratios. The uncertainties are less than 0.3% for both plots.

to measure the plasma density and temperature in the collisional plasmas as accurately as it is done in the solar wind by using the method presented here, along with estimating the collision frequency as third independent parameter, one needs to be aware of the limiting factors that appear in the real environments. In this chapter, we give an overview of "terms and conditions" for applicability of the theory presented above.

3.1. In the Ionosphere of Earth

The main issue for applying the theory given in section 2 is the presence of the magnetic field in the lower ionosphere, having value around several tens of μT and creating electron cyclotron resonance at $\Omega \approx 5 - 7$ MHz. Full adaptation of the QTN spectroscopy to magnetized collisional plasma would assume implementing the solution of Vlasov equation with both magnetic and collision terms included into the theory. This is a very complicated task and is far beyond the scope of this paper. On the other hand, as described below, there are some areas where we actually can obtain a lot of information about the plasma
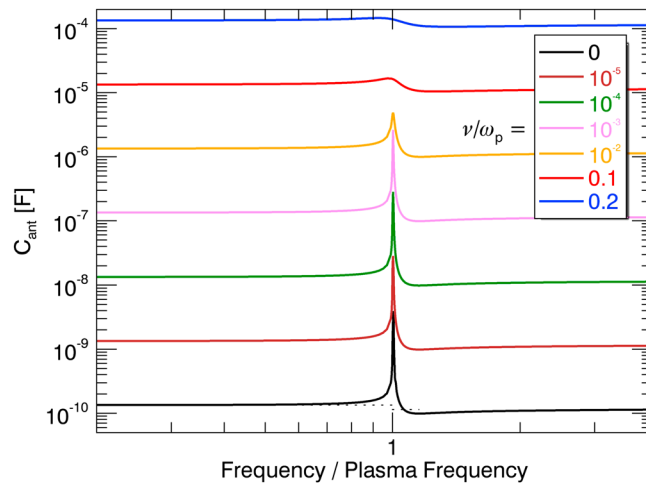

Figure 4. Example of the antenna capacitance of a long dipole antenna ($L_{ant}/L_D = 16$) for different values of the collisional frequency. Dotted points present theoretical limits for low and high frequencies. Results are shifted for a decade for clarity.

parameters by measuring the QTN. In this subsection, we limit our discussion only to low frequencies since for $\omega > \omega_p$ the spectrum is well explained by the hydrodynamic approach [*Balmain*, 1964].

The effects of collisions (in the quiet ionosphere) start becoming notable for $0.01 < \nu/\omega_p$ at ~ 120 km altitude (dayside) [*Bilitza et al.*, 2011], while at $\sim 85–90$ km (approximately the lowest altitude where electron density is still measurable), the collisional effects are expected to be dominant in the QTN spectrum as $\nu/\omega_p \sim 0.5$. In this range of altitudes, the angular plasma frequency of $\omega_p \sim 0.1–5$ MHz and the electron temperature of $T_e \sim 0.02–0.2$ eV are usually measured.

From the numbers given above it is clear that in this region we have $\omega_p < \Omega_e$. The dielectric permittivity function for the magnetized, collisionless, isotropic plasma is given as [*Stix*, 1962]

$$\epsilon\left(\vec{k}, \omega, \vec{B}\right) = 1 + \frac{k_{||}^2}{k_{\perp}^2} + \frac{1}{k_{\perp}^2 L_D^2} \alpha\left(\vec{k}, \omega, \vec{B}\right) \tag{15}$$

with

$$\alpha\left(\vec{k}, \omega, \vec{B}\right) = \sum_{n=-\infty}^{\infty} e^{-\lambda} I_n(\lambda) \left[1 + z_{||} Z_0\left(z_{||} - \frac{n}{r}\right)\right] \tag{16}$$

where $z_{||} = \omega/k_{||} v_{\text{the}}$, $\lambda = \left(k_{\perp} v_{\text{the}}/2\Omega\right)^2$, $r = k_{||} v_{\text{the}}/\Omega$, and I_n is the modified Bessel function. Further on, for a long dipole ($kv_{\text{the}} \ll \omega_p$) at low frequencies we can write $\alpha\left(\vec{k}, \omega, \vec{B}\right)$ as series for small arguments z and λ, along with series of the plasma dispersion function for large argument r^{-1} to obtain

$$\alpha\left(\vec{k}, \omega \rightarrow 0, \vec{B}\right) = 1 + z_{||} Z_0\left(z_{||}\right)(1 + \lambda) \tag{17}$$

On the right-hand side of equation (17) we recognize the solution analogous to one for the unmagnetized plasma, and its correction due to collisions is given in equation (4). Since we know that $kv_{\text{the}} \ll \Omega$, the additional term that scales with λ is negligible, and we conclude that equation (7) stays valid at low frequencies. This is somewhat an expected result since at low frequencies the permittivity is determined by the Debye screening, which is not affected by the magnetic field. For $\omega \sim \omega_p$, equation (17) is not viable, and the QTN theory for magnetized plasma needs to be done in order to interpret the measured spectra.

3.2. Laboratory Plasmas and Unmagnetized Ionospheres

Modern laboratory plasma chambers can operate at very low pressures and mirror the conditions of the lower ionosphere [see, e.g., *Hall and Landauer*, 1971; *Gekelman et al.*, 1991]. Primary purposes of experiments with ionospheric-like plasma devices are studying of spacecraft wakes [*Pigache*, 1973] or ion and neutral flows in ionospheric or tokamak plasmas [*Livesey and Pritchett*, 1989; *Wallace et al.*, 2004].

Besides the diagnostic studies, QTN spectroscopy can be used for precise calibration measurements of plasma parameters in a laboratory device, where the external magnetic field can be completely annulled in the system [*Harp*, 1964; *Graf and Jassby*, 1967]. In these unmagnetized plasmas, the entire QTN spectrum can be used for precise plasma diagnostics—examining the electron temperature and the collision frequency from the low-frequency part of the spectrum, plasma density (with collisional corrections given in section 2.3) from the resonance region and of the electron temperature alone from the high-frequency part. This provides independent measurements of n_e, T_e, and ν with assumption that the plasma VDF is Maxwellian and is, to our knowledge, the only technique able to perform direct precise measurements of the collision frequency in laboratory plasmas by using the wide frequency range, both below and above the plasma frequency. All these features noted for laboratory experiments also stay valid for ionospheres with negligible magnetic field, ones of Mars [*Hanson and Mantas*, 1988; *Acuna et al.*, 1998] and Venus, where the QTN signal around the plasma frequency was clearly observed during the Cassini flyby [*Gurnett et al.*, 2001] (unfortunately on too high altitudes for collisional effects to be noticeable).

On the other hand, the laboratory devices can be used to improve the QTN spectroscopy itself by exploring the antenna response functions. Namely, dipole can be realized with an arbitrary angle and/or with finite gap between the antenna arms, while for real double-sphere antennas, each sphere needs to be placed on a boom. For these irregular geometries, the function F becomes very complicated and in most cases not possible to derive analytically, so it can be calculated from the QTN spectra observed in controlled conditions where

plasma parameters are known. This problem was already discussed during the PIANOS project [*Janhunen et al.*, 2014], and the method proposed here is the way to explore the effects of previously not used antenna geometries.

3.3. Standard Problems and Limitations

If the antenna potential is high compared to the thermal energy of electrons (which is unlikely in the solar wind but can be the case for both ionospheric and laboratory plasmas), then the plasma sheath effects can become significant. This is the problem that has been dealt with in many different ways in the past. The strict kinetic treatment is possible only in the ideal spherical geometry and even then is very complicated [*Buckley*, 1966]. This is the reason why many authors came up with various models of the plasma sheath where the most popular one is the model of the sheath as a cylindrical vacuum region around the dipole and the plasma is assumed to be homogeneous up to the surface of the sheath, studied in detail by *Meyer et al.* [1974]. The simpler model where capacitance of the vacuum sheath is in series with the antenna capacitance is also commonly used, producing satisfying agreement with experimental results [see, e.g., *Balmain*, 1969; *Hall and Landauer*, 1971]. The main issue of all these models is dependence of the sheath thickness, which is itself the unknown parameter that highly affects the results, making the measurements less accurate.

Thus, the most efficient way to go around the complicated sheath issue and obtain best results from the QTN spectroscopy might be the usage of biased antennas with collapsed sheath. In general, the perturbation of the surrounding plasma and attracting/repelling of the particles are depending on the ratio of antenna potential to particles thermal energy [*Laframboise and Parker*, 1973; *Martinović*, 2016], and the sufficient condition for the plasma to be negligibly perturbed by the antenna is this parameter to be close to 0. This condition is achievable in both ionospheric and laboratory plasmas with biased antennas. Good example of this approach is given by *Balmain* [1964], where the experiment with collapsed sheath shows good agreement with the hydrodynamic theory. However, this approach, even though it can be very efficient in laboratory, has a downside when probing the ionospheric plasma. Namely, biasing the antenna abolishes the balance between the fluxes of outgoing photoelectrons and incoming plasma electrons as, instead of the antenna charging, the biasing current makes up for the loss of photoelectrons. This can significantly increase the photoelectron flux and, consequently, the shot noise at low frequencies while the shot noise signal will mostly depend on the value of the zero-potential flux of photoelectrons, that is, on the properties of antenna surface material.

Another potential issue is the current distribution on a wire dipole antenna. In this study the dipole antenna current is assumed to be triangular. This is a valid approximation below the plasma frequency if two conditions are satisfied. First, the antenna is short compared to the free-space wavelength $L_{ant} \ll c/\omega$ [*Balanis*, 1997]. Even though plasma frequency in both ionospheric and laboratory plasmas is several orders of magnitude above the one in the solar wind, this condition is still easily achieved, even for a long dipole ($L_{ant} \gg L_D$) since $v_{the} \ll c$. Second, there are no contributions to the antenna current from electromagnetic surface waves. If $a_{ant} \sim L_D$, then contribution of these waves is considerable, and the current is not triangular [*Meyer et al.*, 1974]. Consequently, the necessary condition $a_{ant} \ll L_D$ [*Couturier et al.*, 1981] dictates usage of very thin antennas (ideally a_{ant} should be at least an order of magnitude below L_D) in all of the described environments.

4. Conclusion

Two main characteristics of the quasi-thermal noise spectroscopy are size and shape of the plasma peak close to the plasma frequency and signal level of the thermal plateau at lower frequencies. The peak is determined by the total plasma density, while the level of the plateau is depending on the electron core temperature. If collisions are present in the plasma, both of these characteristics will be modified, increasing level of the plateau, along with damping and slightly displacing the peak. Since the high-frequency part of the spectrum is unmodified by the collisions, it can be used to deduce the value of the electron temperature in the same manner as it is routinely done in collisionless plasmas. In parallel, precise independent measurements of all n_e, T_e, and ν are available if the collision frequency is $\geq 10\%$ of the plasma frequency as, at this ratio, the low-frequency part of the spectrum is noticeably increased, while the peak damping is clearly visible even for $\nu/\omega_p > 10^{-2}$. The theory presented here can find multiple applications in diagnostic of unmagnetized laboratory plasmas, introducing, for the first time, possibilities to include the low-frequency part of the spectrum in direct measurements of the collisional frequency. The opposite is also possible, as the QTN spectroscopy for cases of different antenna geometries can be studied in controlled environment of a plasma facility. On the other hand, applications in the ionosphere of Earth is strictly limited to very low frequencies due to the

presence of the magnetic field. In order to avoid standard problems that come from affection of the plasma sheath and for the theory to be viable in realistic conditions, we recommend usage of tiny antennas in both space and laboratory measurements. The use of the antenna biasing to reduce the sheath effects can be promising but should be investigated in more details.

References

Acuna, M. H., et al. (1998), Magnetic field and plasma observations at Mars: Initial results of the Mars Global Surveyor mission, *Science*, *279*, 1676–1680.

Alexandrov, A. F., L. S. Bogdankevich, and A. A. Rukhadze (1984), *Principles of plasma electrodynamics*, Springer, Berlin.

Balanis, C. A. (1997), *Antenna Theory; Analysis and Design*, Wiley, Hoboken, N. J.

Balmain, K. (1964), The impedance of a short dipole antenna in a magnetoplasma, *IEEE Trans. Antenn. Propag.*, *12*, 605–617.

Balmain, K. (1969), Dipole admittance for magnetoplasma diagnostics, *IEEE Trans. Antenn. Propag.*, *17*, 389–392.

Bhatnagar, P. L., E. P. Gross, and M. Krook (1954), A model for collision processes in gases. I. Small amplitude processes in charged and neutral one-component systems, *Phys. Rev.*, *94*, 511–525.

Bilitza, D., L.-A. McKinnell, B. Reinisch, and T. Fuller-Rowell (2011), The international reference ionosphere today and in the future, *J. Geod.*, *85*, 909–920.

Blackwell, D. D., D. N. Walker, S. J. Messer, and W. E. Amatucci (2007a), Antenna impedance measurements in a magnetized plasma. I. Spherical antenna, *Phys. Plasmas*, *14*, 92105.

Blackwell, D. D., D. N. Walker, S. J. Messer, and W. E. Amatucci (2007b), Antenna impedance measurements in a magnetized plasma. II. Dipole antenna, *Phys. Plasmas*, *14*, 92106.

Buckley, R. (1966), A theory of resonance rectification. The response of a spherical plasma probe to alternating potentials, *Proc. R. Soc. A*, *290*, 186–219.

Chateau, Y. F., and N. Meyer-Vernet (1991), Electrostatic noise in non-Maxwellian plasmas: Generic properties and 'kappa' distributions, *J. Geophys. Res.*, *96*, 5825–5836.

Couturier, P., N. Meyer-Vernet, S. Hoang, and J. L. Steinberg (1981), Quasi-thermal noise in a stable plasma at rest: Theory and observations from ISEE 3, *J. Geophys. Res.*, *86*, 11,127–11,138.

Fried, B. D., and S. D. Conte (1961), *The Plasma Dispersion Function*, Acad. Press, New York.

Gekelman, W., H. Pfister, Z. Lucky, J. Bamber, D. Leneman, and J. Maggs (1991), Design, construction, and properties of the large plasma research device – The LAPD at UCLA, *Rev. Sci. Instrum.*, *62*, 2875–2883.

Graf, K. A., and D. L. Jassby (1967), Measurements of dipole antenna impedance in an isotropic laboratory plasma, *IEEE Trans. Antenn. Propag.*, *5*, 681–688.

Gurnett, D. A., P. Zarka, R. Manning, W. S. Kurth, G. B. Hospodarsky, T. F. Averkamp, M. L. Kaiser, and W. M. Farrell (2001), Non-detection at venus of high-frequency radio signals characteristic of terrestrial lightning, *Nature*, *409*, 313–315.

Hall, T. A., and G. Landauer (1971), Admittance of dipolar RF probes in a simulated ionosphere, *Radio Sci.*, *6*, 967–980.

Hanson, W. B., and G. P. Mantas (1988), Viking electron temperature measurements – Evidence for a magnetic field in the Martian ionosphere, *J. Geophys. Res.*, *93*, 7538–7544.

Harp, R. S. (1964), The behavior of the resonance probe in a plasma, *Appl. Phys. Lett.*, *4*, 186–188.

Hoang, S. (1972), Admittance measurements of a 36-m dipole antenna in the topside ionosphere, *Planet. Space Sci.*, *20*, 1185–1204.

Issautier, K., N. Meyer-Vernet, M. Moncuquet, and S. Hoang (1999), Quasi-thermal noise in a drifting plasma: Theory and application to solar wind diagnostic on Ulysses, *J. Geophys. Res.*, *104*, 6691–6704.

Janhunen, P., K. Issautier, and H. Lamy, (2014), PIANOS: Plasma induced antenna noise spectroscopy for space weather plasma measurements, Final Rep. 4000108571/13/NL/MV, ESA/ESTEC, Noordwijk, Netherlands.

Kuehl, H. H. (1966), Resistance of a short antenna in a warm plasma, *Radio Sci.*, *1*, 971–976.

Laframboise, J. G., and L. W. Parker (1973), Probe design for orbit-limited current collection, *Phys. Fluids*, *16*, 629–636.

Le Chat, G., K. Issautier, N. Meyer-Vernet, and S. Hoang (2011), Large-scale variation of solar wind electron properties from quasi-thermal noise spectroscopy: Ulysses measurements, *Sol. Phys.*, *271*, 141–148.

Livesey, W. A., and P. L. Pritchett (1989), Two-dimensional simulations of a charge-neutral plasma beam injected into a transverse magnetic field, *Phys. Fluids B*, *1*, 914–922.

Martinović, M. M. (2016), Orbit limited theory in the solar wind – κ distributions, *Serb. Astron. J.*, *192*, 27–34.

Meyer, P., N. Vernet, and P. Lassudrie-Duchesne (1974), Theoretical and experimental study of the effect of the sheath on an antenna immersed in a warm isotropic plasma, *J. Appl. Phys.*, *45*, 700–706.

Meyer-Vernet, N. (1979), On natural noises detected by antennas in plasmas, *J. Geophys. Res.*, *94*, 2405–2415.

Meyer-Vernet, N. (1983), Quasi-thermal noise correction due to particle impacts of emission, *J. Geophys. Res.*, *88*, 8081–8093.

Meyer-Vernet, N., and C. Perche (1989), Tool kit for antennae and thermal noise near the plasma frequency, *J. Geophys. Res.*, *94*, 2405–2415.

Moncuquet, M., A. Lecacheux, N. Meyer-Vernet, B. Cecconi, and W. S. Kurth (2005), Quasi thermal noise spectroscopy in the inner magnetosphere of saturn with CASSINI/RPWS: Electron temperatures and density, *Geophys. Res. Lett.*, *32*, L20S02, doi:10.1029/2005GL022508.

Nakatani, D. T., and H. H. Kuehl (1976), Input impedance of a short dipole antenna in a warm anisotropic plasma, 1, kinetic theory, *Radio Sci.*, *11*, 433–444.

Nyquist, H. (1928), Thermal agitation of electric charge in conductors, *Phys. Rev.*, *32*, 110–113.

Pigache, D. W. (1973), A laboratory simulation of the ionospheric plasma, *Am. Inst. Aeronaut. Astronaut. J.*, *11*, 129–130.

Schelkunoff, S. A., and H. T. Friis (1952), *Antennas: Theory and Practice*, Wiley, Hoboken, N. J..

Schiff, M. L. (1970), Impedance of a short dipole antenna in a warm isotropic plasma, *Radio Sci.*, *5*, 1489–1496.

Spencer, E., and S. Patra (2015), Ionosphere plasma electron parameters from radio frequency sweeping impedance probe measurements, *Radio Sci.*, *50*, 853–965.

Stix, T. H. (1962), *The Theory of Plasma Waves*, McGraw-Hill, Pa.

Wallace, E., E. Thomas, A. Eadon, and J. D. Jackson (2004), Design and initial operation of the Auburn Linear Experiment for Instability Studies: A new plasma experiment for studying shear driven flows, *Rev. Sci. Instrum.*, *75*, 5160–5165.